

FAST RADIO BURSTS: COLLISIONS BETWEEN NEUTRON STARS AND ASTEROIDS/COMETS

J. J. Geng^{1,2}, and Y. F. Huang^{1,2}

ABSTRACT

Fast radio bursts (FRBs) are newly discovered radio transient sources. Their high dispersion measures indicate a cosmological origin. But due to the lack of observational data in other wavelengths, their progenitors still remain unclear. Here we suggest the collisions between neutron stars and asteroids/comets as a promising mechanism for FRBs. During the impact process, a hot plasma fireball will form after the material of the small body penetrates into the neutron star surface. The ionized matter inside the fireball will then expand along the magnetic field lines. Coherent radiation from the thin shell at the top of the fireball will account for the observed FRBs. Our scenario can reasonably explain the main features of FRBs, such as their durations, luminosities, and the event rate. We argue that for a single neutron star, FRBs are not likely to happen repeatedly in a foreseeable time span since such impacts are of low probability. We predict that faint X-ray afterglows should be associated with FRBs, which may be detected by future rapid follow-up observations of FRBs.

Subject headings: pulsars: general — radio continuum: general — stars: neutron — minor planets, asteroids: general

1. INTRODUCTION

Recently, the discovery of a number of fast radio bursts (FRBs) was reported (Lorimer et al. 2007; Thornton et al. 2013). Typically, they are single radio pulses with flux densities $S_\nu \sim$ a few Jy and durations $\delta t \sim$ a few ms at frequency $\nu_{\text{FRB}} \sim 1$ GHz. There have been no counterparts observed in other wavelengths till now (Petroff et al. 2014), maybe due to the lack of rapid, multiwavelength follow-up after the bursts. According to their

¹School of Astronomy and Space Science, Nanjing University, Nanjing 210046, China; hyf@nju.edu.cn

²Key Laboratory of Modern Astronomy and Astrophysics (Nanjing University), Ministry of Education, Nanjing 210046, China

high dispersion measures ($\sim 500 - 1000 \text{ cm}^{-3} \text{ pc}$), FRBs are increasingly believed to be at cosmological distances with redshifts $0.5 \leq z \leq 1$ (Thornton et al. 2013; Luan & Goldreich 2014). Consequently, the characteristic isotropic radio luminosity (L_{FRB}) is estimated to be $\sim 10^{42-43} \text{ erg s}^{-1}$ and the isotropic energy (E_{FRB}) released is then 10^{39-40} erg . The observational event rate of FRBs is suggested to be $\sim 10^{-3} \text{ gal}^{-1} \text{ yr}^{-1}$ (Thornton et al. 2013; Keane & Petroff 2015).

The central engines of FRBs are under hot debate. The durations of FRBs indicate the emission regions are compact, while the high brightness of the radio emission requires coherent emission to take effect (Katz 2014a), which is similar to radio emissions from pulsar magnetospheres (Ruderman & Sutherland 1975; Cheng & Ruderman 1977; Benford & Buschauer 1977). Also, the energy reservoir in a neutron star (NS) magnetosphere is high enough to account for the energy release of FRBs. These few but significant clues motivate some authors to associate FRBs with scenarios involving NSs. Several possible models have been proposed, e.g., magnetar giant flares (Kulkarni et al. 2014; Lyubarsky 2014; Pen & Connor 2015), collapse of hypermassive neutron stars (NSs) into black holes (Falcke & Rezzolla 2014; Zhang 2014; Ravi & Lasky 2014), binary NS mergers (Totani 2013) and planetary companions around NSs (Mottez & Zarka 2014). At the same time, other kinds of models have also been proposed, e.g., binary white dwarf mergers (Kashiyama et al. 2013), flare stars (Loeb et al. 2014) and evaporation of primordial black holes (Barrau et al. 2014).

However, besides the above scenarios, there may be another external way to trigger the energy release in the NS magnetosphere. It has previously been suggested in the literature that small solid bodies such as asteroids or comets can impact NSs occasionally (Mitrofanov & Sagdeev 1990; Colgate & Petschek 1981; Huang & Geng 2014). It is interesting to notice that the timescale and energy release of these impacts can meet the requirements of FRB progenitors from the first view. Additionally, the event rate for these considerable strong impacts seems to be consistent with that of the observational FRBs. Thus we suggest that the impacts between NSs and comets/asteroids may provide a possible explanation for FRBs. In this Letter, we briefly describe the impact process in Section 2. In Section 3, we present the formulas for the radiation process and derive the basic features of the emission. In Section 4, the afterglow emission in our scenario is discussed. Our conclusions are summarized in Section 5.

2. IMPACT PROCESS

Direct impacts between asteroids/comets and NSs have been previously discussed in different contexts. In order to give a quantitative description of our model, here we would

like to give a brief review of the impact process, mainly following the study in Colgate & Petschek (1981). When a small solid body of mass m falls freely in the gravitational field of an isolated NS of mass M , it will undergo elongation in the radial direction. The elongated body will be broken up at the breakup radius and the collapsed material will be compressed by the magnetic field of the NS before landing. For an Fe-Ni asteroid with a density ρ_0 , radius r_0 , and shear strength s , the breakup radius of the elongated body is

$$R_b = (\rho_0 r_0^2 M G / s)^{1/3}, \quad (1)$$

where G is the gravitational constant. We assume the leading fragment (at $R_b - r_0$) and lagging portion (at $R_b + r_0$) have the same velocity v_b (v_b is determined from the free fall assumption from $R = \infty$) when the asteroid center is at R_b . The subsequent free fall gives the evolution of the velocities of the leading and lagging fragments (v_- and v_+) as

$$\frac{1}{v_{\pm}} \approx \left(\frac{2GM}{R} \right)^{-1/2} \left(1 \pm \frac{r_0 R}{2R_b^2} \right). \quad (2)$$

The difference of arrival time at the surface of the NS (R_{NS}) is then

$$\begin{aligned} \Delta t_a &= \int_{R_{\text{NS}}}^{R_b+r_0} \frac{dR}{v_+} - \int_{R_{\text{NS}}}^{R_b-r_0} \frac{dR}{v_-} \simeq 2r_0/v_b = 2r_0 \left(\frac{2GM}{R_b} \right)^{-1/2} \\ &= 1.58 \times 10^{-3} m_{18}^{4/9} s_{10}^{-1/6} \left(\frac{\rho_0}{8 \text{ g cm}^{-3}} \right)^{-5/18} \left(\frac{M}{1.4 M_{\odot}} \right)^{-1/3} s, \end{aligned} \quad (3)$$

where the convention $Q_x = Q/10^x$ in cgs units is adopted hereafter. This impact time scale is less than the duration of the observed FRBs, so the short-time characteristic of FRBs can basically be met in our model.

When approaching the NS surface, the accretion column will penetrate the magnetic field as a compressed sheet of diamagnetic fluid with all magnetic field lines parallel to its surface. The compression in longitude reduces the thickness of the sheet to a few millimeters, while its width in latitude would expand to a few kilometers at the NS surface. The dense matter then plunges into the NS outer crust and the kinetic energy is converted to thermal energy, launching a rapidly expanding plasmoid fireball along the field lines (see Figure 1 for a schematic illustration). A fan of field lines are finally filled with hot plasma (see Colgate & Petschek (1981) for details). In the plasma, plenty of electrons are accelerated to ultra-relativistic speeds by magnetic reconnection near the collision site. Radiation from this fan of hot plasma will give birth to an observable FRB, as detailed in the following section.

3. EMISSION MECHANISM

The high brightness temperatures of FRBs indicate they are from the coherent emission. This radiation mechanism may also be involved in radio emission of pulsars. Although the progenitors of FRBs are still uncertain, some constraints on the emission region can be derived from observations (Katz 2014b). In our scenario, the hot plasma fan can produce the required coherent emission (see Figure 1). The electron bunches originated from the collision will form a shell with a thickness of Δ at r_{emi} from the NS. The duration δt of FRBs implies $\Delta \approx c\delta t$. The emission volume of this shell is $V_{\text{emi}} \approx 4\pi f\Delta r_{\text{emi}}^2$. Note that f is the ratio of the shell solid angle to 4π . At the bottom of the fan, the thickness in longitude is $\sim 10^4$ cm as a result of the turbulent expansion, thus $f \approx \frac{10^4 \text{ cm}}{2\pi R_{\text{NS}}} = 3 \times 10^{-3}$. Electrons radiate coherently in patches with a characteristic radial size of $\lambda = c/\nu_c$ (ν_c is the characteristic frequency of curvature emission), the corresponding volume of each patch is $V_{\text{coh}} = (4/\gamma^2) r_{\text{emi}}^2 \times (c/\nu_c)$. Here the factor $4/\gamma^2$ is the solid angle within which electrons can be casually connected in the relativistic beam.

The coherent curvature emission luminosity can be estimated as (Kashiyama et al. 2013)

$$L_{\text{tot}} \approx (P_e N_{\text{coh}}^2) \times N_{\text{pat}}, \quad (4)$$

where $P_e = 2\gamma^4 e^2 c / 3r_{\text{emi}}^2$ is the emission power of a single electron, $N_{\text{coh}} \approx n_e \times V_{\text{coh}}$ is the number of electrons in each coherent patch, and $N_{\text{pat}} \approx V_{\text{emi}}/V_{\text{coh}}$ is the number of the patches. The characteristic frequency of curvature emission is

$$\nu_c = \gamma^3 \frac{3c}{4\pi r_{\text{emi}}}. \quad (5)$$

On the other hand, since the electrons are bound to the field lines, it is reasonable to assume that the energy density of electrons is in equilibrium with the magnetic energy density at r_{emi} . Thus we have $B^2(r_{\text{emi}})/8\pi = \epsilon n_e \gamma m_e c^2$, where the parameter ϵ is introduced to describe the deviation from such an equilibrium. Here the magnetic field strength can be estimated as $B(r_{\text{emi}}) \approx B_{\text{NS}} \times (r_{\text{emi}}/R_{\text{NS}})^{-3}$, where B_{NS} is the surface magnetic field strength at R_{NS} .

Using the formulas above and assuming $L_{\text{tot}} = fL_{\text{FRB}}$, $\nu_c = \nu_{\text{FRB}}$, we can solve out the typical Lorentz factor of electrons in the emitting shell as

$$\gamma \simeq 547 \left(\epsilon_0^{-2} B_{\text{NS},12}^4 R_{\text{NS},6}^{12} \delta t_{-2} \nu_{\text{FRB},9}^9 L_{\text{FRB},42}^{-1} \right)^{1/30}. \quad (6)$$

The corresponding typical values of other quantities are $r_{\text{emi}} \simeq 1.2 \times 10^9$ cm, $\Delta \simeq 3 \times 10^8$ cm, $B(r_{\text{emi}}) \simeq 580$ G, and $n_e \simeq 3 \times 10^7$ cm $^{-3}$. It is worthy to note that n_e actually refers

to the number density of electrons and positrons generated from photon pair production. Therefore, it could be significantly larger than the Goldreich-Julian density (Goldreich & Julian 1969).

For the radio emission propagating through the plasma, it is essential that the characteristic plasma frequency must be below the frequency of the propagating radio waves, i.e.,

$$\nu_p = \gamma \left(\frac{n'_e e^2}{\pi m_e} \right)^{1/2} \leq \nu_{\text{FRB}}, \quad (7)$$

where $n'_e = n_e/\gamma$ is the number density of electrons in the comoving frame. Using the parameters derived above, we find this requirement can be satisfied.

In general, both the gravitational potential energy of the asteroid and the magnetic field energy of the NS can provide the energy emitted. If all the energy released is contributed by the former one, i.e.,

$$f E_{\text{FRB}} = \eta \frac{GMm}{R_{\text{NS}}}, \quad (8)$$

then the mass needed is $m = 5.4 \times 10^{18} \eta_{-1}^{-1} f_{-2} E_{\text{FRB},40} R_{\text{NS},6} M_{1.4M_\odot}^{-1}$ g, where η is the efficiency of transforming the potential energy into radiation. This mass is roughly in the mass range of normal asteroids, assuring the self-consistency of our model.

4. AFTERGLOWS

No counterparts associated with FRBs have been observed till now, making FRBs more mysterious. A recent multiwavelength follow-up to FRB 140514 reveals no variable counterparts or transient emissions associated with it (Petroff et al. 2014). There are two possible reasons for this mysterious fact. On one hand, the progenitors of FRBs may be such transient sources so the duration of signals in other bands are also too short, beyond the reaction capability of telescopes in search. On the other hand, the flux of FRB counterparts may be very weak and be below the detection limit of the telescopes. In our scenario, the matter collapsed onto the NS surface may contribute to emissions in other bands. It is interesting to discuss whether the afterglows following the bursts can be detected by detectors at work.

While some electrons are accelerated to move to the top of the fan, most of the matter collapsed would remain in a column on the NS surface. The temperature of this matter is high during the impact, and would decrease later when it loses its energy by radiation. Although the cooling process of the hot matter is not clearly known, we can have a rough estimate on the basis of reasonable assumptions. After the giant flare of 1998 August 27, transient

X-ray emission decaying as $\propto t^{-0.7}$ was observed from SGR 1900+14. It was suggested to be the cooling behavior of the heated crust of magnetar (Lyubarsky et al. 2002). In our model, we assume that the heated matter releases its energy mainly in X-ray band at early time ($\leq 10^6$ s) and the cooling obeys the same decaying law. The peak X-ray flux is then the key uncertain parameter. In order to give a simple estimate, we can calculate the X-ray flux at 10 ms (just after the burst). It can be determined from the thermal radiation. Thus, for a FRB at a luminosity distance d_L , the X-ray afterglow light curve is

$$F_X \approx \sigma T^4 \left(\frac{R_{\text{NS}}}{d_L} \right)^2 \left(\frac{t}{0.01\text{s}} \right)^{-0.7}, \quad (9)$$

where σ is the Stefan-Boltzmann constant and T is the temperature of the matter. The temperature can reach ~ 100 keV according to Colgate & Petschek (1981) and we adopt this value in our calculations. Figure 2 presents the light curves from sources at different redshifts, together with the sensitivity line of the *Swift*/X-Ray Telescope (Moretti et al. 2009; Burrows et al. 2014; Yi et al. 2014). It can be seen that unless the FRB is at low redshift ($z \leq 0.01$), its X-ray counterpart will be difficult to detect.

Other factors, e.g., the spreading of the collapsed matter on the NS surface, and the rotation of the NS, would reduce the flux significantly and are not considered here. The calculation above is actually an optimistic estimate. Therefore, the counterparts associated with FRBs may be even more difficult to observe.

5. SUMMARY AND DISCUSSION

In this study, we propose that the impacts between NSs and asteroids/comets may be a promising mechanism for FRBs. For an asteroid of typical mass of 10^{18} g falling onto the NS surface, a fan of hot plasma would form after the millisecond collision. The consequent emitting shell at $r_{\text{emi}} \sim 1.2 \times 10^9$ cm, containing electrons/positrons with $\gamma \approx 550$, will emit in radio wavelength coherently. The main characteristics of FRBs, including the timescale and luminosity, can be well explained in our scenario.

Moreover, the X-ray afterglows following the FRBs will be faint according to the calculations from reasonable assumptions. Unless the FRB is at low redshift ($z \leq 0.01$), the X-ray afterglow will be hard to detect. Till now, no repeating bursts have been observed from any particular FRB sources. This feature can be naturally explained in our scenario since a direct collision between an asteroid/comet and the NS can only trigger the burst once, and such collisions are not likely to happen repeatedly on short timescales. These predictions make our model testable by more observations in the future.

The event rate of FRBs is another crucial clue to the progenitors. Although it is difficult to assess the exact event rate of the impact processes, we can give a rough estimate on the basis of reasonable assumptions. The planetary system of an NS can be retained during the violent supernova explosion that gives birth to it (Wolszczan & Frail 1992). The pre-supernova Oort-like cometary cloud may also remain. In previous articles, for a NS traveling in its pre-supernova Oort-like cometary cloud, the recurrence time τ_{rec} of strong direct impacts is $\sim 10^7$ years (Mitrofanov & Sagdeev 1990; Tremaine & Zytkov 1986; Litwin & Rosner 2001). Supposing the number of NSs in a typical galaxy is 10^8 (Timmes et al. 1996), then the observable event rate of the impact is $\zeta \approx f \frac{10^8/\text{galaxy}}{10^7\text{yr}} = 10^{-2} f_{-3} \text{ gal}^{-1} \text{ yr}^{-1}$. Recently the Alfvén wing structures formed during the interaction between a relativistic pulsar wind and the orbiting small body were investigated. It was found that the Alfvén wing structures will lead the small bodies in a retrograde orbit to move toward the central NS more rapidly (Mottez & Heyvaerts 2011), which can markedly increase the collision rate. However, the very limited field of view of current large radio telescopes makes the observation of FRBs very difficult. Considering these, the anticipated event rate would be consistent with the observed FRB rate.

A key to reveal the nature of FRBs may be the coherent curvature emission. In fact, what we have proposed is one kind of process that can trigger the coherent emission from the magnetosphere of NS. The conditions needed to drive the particle bunching, which may involve some kinds of instabilities, is still unclear and is beyond the scope of our work. Future advance in the study of coherent radiation could give more rigorous clue to the progenitors of FRBs.

We thank Shuang-Xi Yi and Wei Su for helpful discussions. This study was supported by the National Basic Research Program of China with Grant No. 2014CB845800, and by the National Natural Science Foundation of China with Grant No 11473012.

REFERENCES

- Barrau, A., Rovelli, C., & Vidotto, F. 2014, *Phys. Rev. D*, 90, 127503
- Benford, G., & Buschauer, R. 1977, *MNRAS*, 179, 189
- Burrows, D. N., Frank, K. A., & Park, S. 2014, *BAAS*, 223, 353.14
- Cheng, A. F., & Ruderman, M. A. 1977, *ApJ*, 212, 800
- Colgate, S. A., & Petschek, A. G. 1981, *ApJ*, 248, 771

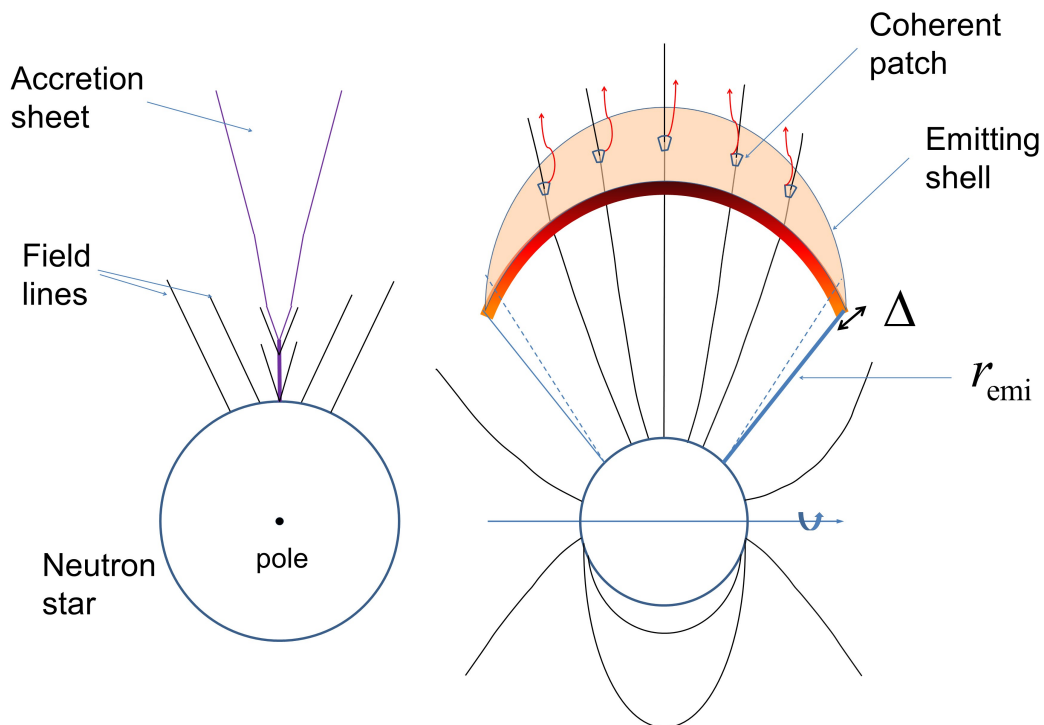


Fig. 1.— Schematic illustration of the impact between a NS and an asteroid/comet. The left panel shows the elongated body is accreted onto the NS as a sheet (see Colgate & Petschek (1981) for a detailed plot). The magnetic compression in longitude reduces its thickness to a few millimeters, while the width in latitude would expand to a few kilometers when approaching the NS surface. The right panel depicts the hot plasma fan generated shortly after the collision. The emitting shell (red-orange arc) is the region where the coherent curvature radiation is generated.

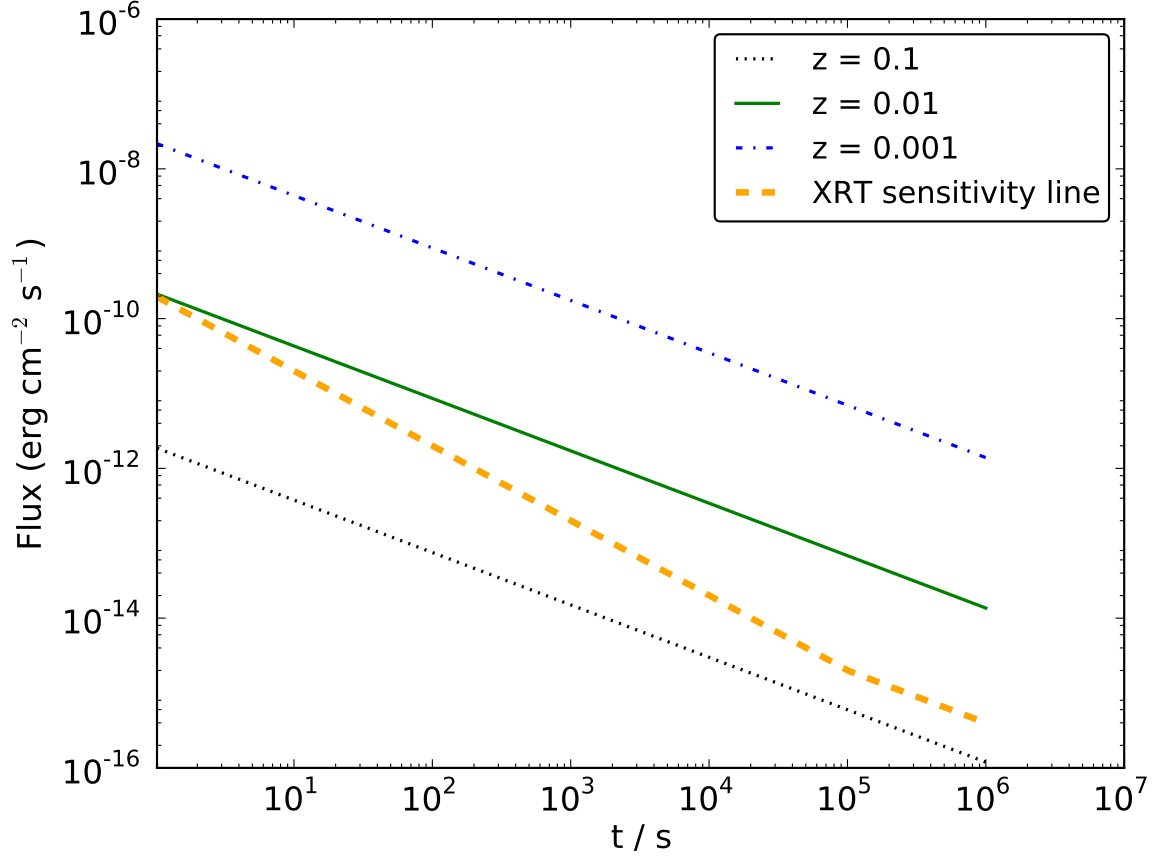


Fig. 2.— Predicted X-ray afterglow light curves after the FRBs in our scenario. Three values of redshifts $z = 0.1$ (dotted line), 0.01 (solid line), 0.001 (dash-dotted line) are adopted. The thick dashed line is the sensitivity line of the *Swift*/X-Ray Telescope (Moretti et al. 2009; Burrows et al. 2014; Yi et al. 2014). Note that for the sensitivity line, the x-axis is the integration time, while the y-axis is the corresponding sensitivity limit under this exposure time.

- Falcke, H., & Rezzolla, L. 2014, *A&A*, 562, A137
- Goldreich, P., & Julian, W. H. 1969, *ApJ*, 157, 869
- Huang, Y. F., & Geng, J. J. 2014, *ApJ*, 782, L20
- Kashiyama, K., Ioka, K., & Mészáros, P. 2013, *ApJ*, 776, L39
- Katz, J. I. 2014a, *Phys. Rev. D*, 89, 103009
- Katz, J. I. 2014b, arXiv:1409.5766
- Keane, E. F., & Petroff, E. 2015, *MNRAS*, 447, 2852
- Kulkarni, S. R., Ofek, E. O., Neill, J. D., Zheng, Z., & Juric, M. 2014, *ApJ*, 797, 70
- Litwin, C., & Rosner, R. 2001, *Physical Review Letters*, 86, 4745
- Loeb, A., Shvartzvald, Y., & Maoz, D. 2014, *MNRAS*, 439, L46
- Lorimer, D. R., Bailes, M., McLaughlin, M. A., Narkevic, D. J., & Crawford, F. 2007, *Science*, 318, 777
- Luan, J., & Goldreich, P. 2014, *ApJ*, 785, L26
- Lyubarsky, Y. 2014, *MNRAS*, 442, L9
- Lyubarsky, Y., Eichler, D., & Thompson, C. 2002, *ApJ*, 580, L69
- Mitrofanov, I. G., & Sagdeev, R. Z. 1990, *Nature*, 344, 313
- Moretti, A., Pagani, C., Cusumano, G., et al. 2009, *A&A*, 493, 501
- Mottez, F., & Heyvaerts, J. 2011, *A&A*, 532, A22
- Mottez, F., & Zarka, P. 2014, *A&A*, 569, A86
- Pen, U.-L., & Connor, L. 2015, arXiv:1501.01341
- Petroff, E., Bailes, M., Barr, E. D., et al. 2014, *MNRAS* accepted
- Ravi, V., & Lasky, P. D. 2014, *MNRAS* accepted
- Ruderman, M. A., & Sutherland, P. G. 1975, *ApJ*, 196, 51
- Thornton, D., Stappers, B., Bailes, M., et al. 2013, *Science*, 341, 53

Timmes, F. X., Woosley, S. E., & Weaver, T. A. 1996, *ApJ*, 457, 834

Totani, T. 2013, *PASJ*, 65, L12

Tremaine, S., & Zytlow, A. N. 1986, *ApJ*, 301, 155

Wolszczan, A., & Frail, D. A. 1992, *Nature*, 355, 145

Yi, S.-X., Gao, H., & Zhang, B. 2014, *ApJ*, 792, L21

Zhang, B. 2014, *ApJ*, 780, L21